

# Solution Structure and Functional Analysis of the Cysteine-rich C1 Domain of Kinase Suppressor of Ras (KSR)

Ming Zhou<sup>1</sup>, David A. Horita<sup>2</sup>, David S. Waugh<sup>3</sup>, R. Andrew Byrd<sup>2</sup> and Deborah K. Morrison<sup>1\*</sup>

<sup>1</sup>*Regulation of Cell Growth Laboratory*

<sup>2</sup>*Structural Biophysics Laboratory*

<sup>3</sup>*Macromolecular Crystallography Laboratory, National Cancer Institute, Frederick Cancer Research and Development Center, Frederick MD 21702, USA*

Kinase suppressor of Ras (KSR) is a conserved component of the Ras pathway that acts as a molecular scaffold to promote signal transmission from Raf-1 to MEK and MAPK. All KSR proteins contain a conserved cysteine-rich C1 domain, and studies have implicated this domain in the regulation of KSR1 subcellular localization and function. To further elucidate the biological role of the KSR1 C1 domain, we have determined its three-dimensional solution structure using nuclear magnetic resonance (NMR). We find that while the overall topology of the KSR1 C1 domain is similar to the C1 domains of Raf-1 and PKC $\gamma$ , the predicted ligand-binding region and the surface charge distribution are unique. Moreover, by generating chimeric proteins in which these domains have been swapped, we find that the C1 domains of Raf-1, PKC $\gamma$ , and KSR1 are not functionally interchangeable. The KSR1 C1 domain does not bind with high affinity or respond biologically to phorbol esters or ceramide, and it does not interact directly with Ras, indicating that the putative ligand(s) for the KSR1 C1 domain are distinct from those that interact with PKC $\gamma$  and Raf-1. In addition, our analysis of the chimeric proteins supports the model that Raf-1 is a ceramide-activated kinase and that its C1 domain is involved in the ceramide-mediated response. Finally, our findings demonstrate an absolute requirement of the KSR1 C1 domain in mediating the membrane localization of KSR1, a crucial feature of its scaffolding activity. Together, these results underscore the functional specificity of these important regulatory domains and demonstrate that the structural features of the C1 domains can provide valuable insight into their ligand-binding properties.

*Keywords:* KSR; cysteine-rich C1 domain; MAPK cascade; signal transduction; NMR structure

\*Corresponding author

---

Present address: D. A. Horita, Department of Biochemistry, Wake Forest University School of Medicine, Medical Center Blvd, Winston-Salem, NC 27157, USA.

Abbreviations used: KSR, kinase suppressor of Ras; PKC, protein kinase C; MAPK, mitogen-activated protein kinase; MEK, MAP or ERK kinase; GST, glutathione-S-transferase; WT, wild-type; PDGF, platelet-derived growth factor; TPA, 12-O-tetradecanoyl-phorbol-13-acetate; HSQC, heteronuclear single quantum coherence; NOE, nuclear Overhauser effect; NOESY, NOE spectroscopy; RMSD, root-mean-square deviation; TEV, tobacco etch virus; GVBD, germinal

E-mail address of the corresponding author: [dmorrison@ncitcr.gov](mailto:dmorrison@ncitcr.gov)

## Introduction

The Ras pathway is an essential signal transduction cascade involved in cell proliferation, transformation, differentiation, and apoptosis.<sup>1</sup> Although this pathway has been studied extensively for more than a decade, there are still numerous aspects of Ras signaling that have not been elucidated fully. In particular, the level of cross-talk between various Ras effectors is unclear, as is the function and regulation of some pathway components. One member of the Ras pathway that has been particularly enigmatic is kinase suppressor of Ras (KSR).

KSR represents a unique protein family that was first identified to be a positive regulator of Ras sig-

naling by genetic studies performed in *Drosophila melanogaster* and *Caenorhabditis elegans*.<sup>2-4</sup> Members of the KSR family contain five conserved protein domains (termed CA1-5) and display remarkable overall sequence similarity to proteins of the Raf kinase family.<sup>2</sup> The conserved KSR domains include a 40 residue region unique to KSR proteins (CA1), a proline-rich region (CA2), a cysteine-rich C1 domain (CA3), a serine/threonine-rich region (CA4), and a putative kinase domain (CA5). Similar to the domain organization of Raf-1, the smaller conserved domains of KSR1 are found in the N-terminal region, while the kinase-like domain occupies the C-terminal half of the protein. Unlike Raf-1, however, the kinase domain of KSR1 appears to be non-functional, suggesting that KSR1 does not promote Ras signaling by phosphorylating target molecules.<sup>2,5,6</sup> A growing body of evidence now indicates that a primary function of KSR1 is as a scaffolding protein that coordinates the assembly of a membrane-bound multiprotein complex containing MAPK and its upstream regulators, MEK and Raf-1.<sup>5,7-11</sup>

A region of KSR1 that appears to be critical for its function is the CA3 cysteine-rich C1 domain. KSR1 proteins that either lack this domain or contain mutations in its conserved cysteine residues are unable to facilitate Ras signaling.<sup>7,12</sup> Moreover, mutation of the cysteine residues prevents the Ras-dependent localization of KSR1 to membrane fractions.<sup>12</sup> Cysteine-rich C1 domains are found in numerous proteins involved in signal transduction, including protein kinase C enzymes (PKC) and Raf-1, and have been classified into two groups, termed typical and atypical.<sup>13</sup> Typical C1 domains interact with diacylglycerol and phorbol esters, whereas the atypical C1 domains do not. The KSR1 C1 domain falls into the atypical class and shares the highest degree of sequence homology to the atypical C1 domain found in Raf-1. C1 domains, whether typical or atypical, have been shown to play key roles in regulating the function of the proteins in which they are found.<sup>13</sup>

To further elucidate the biological role of the KSR1 C1 domain, we have determined its three-dimensional structure and have compared the structure and function of this domain with the C1 domains present in Raf-1 and PKC $\gamma$ . We find that each of these domains is structurally distinct, even though the overall folding pattern is similar. Distinguishing features of the different C1 domains are most apparent in the predicted ligand-binding regions. These differences apparently contribute to the binding specificities of the individual C1 sequences and account for the inability of these domains to functionally replace one another. Finally, we find that the KSR1 C1 domain is essential for the translocation and stable accumulation of KSR1 at the plasma membrane, presumably reflecting the interaction of the KSR1 C1 domain with as yet unidentified membrane-bound ligand(s).

## Results and Discussion

### Solution structure of the KSR1 C1 domain

C1 domains are defined as regions of approximately 50 amino acid residues that contain the motif HX<sub>10-12</sub>CX<sub>2</sub>CX<sub>11-19</sub>CX<sub>2</sub>CX<sub>4</sub>HX<sub>2-4</sub>CX<sub>5-9</sub>C. The KSR1 C1 domain (residues 334 to 377) was expressed as a glutathione-S-transferase (GST) fusion protein in *Escherichia coli*. After initial purification using glutathione beads, the C1 domain was cleaved from GST and further purified to homogeneity. <sup>1</sup>H and <sup>15</sup>N resonance assignments of the KSR1 C1 domain were made using standard two-dimensional and three-dimensional NMR techniques. Statistics for the KSR1 C1 structure are detailed in Table 1. The final structure was based on the analysis of 20 lowest-energy structures from an ensemble of 200 structures. As depicted in the stereo-diagram presented in Figure 1, the overall structure of the KSR1 C1 domain consists of two anti-parallel  $\beta$ -sheets and a C-terminal helix turn. The first  $\beta$ -sheet forms the core of the C1 structure and consists of three strands,  $\beta$ 1 (residues 333-339),

**Table 1.** Structural statistics

Restrains		
NOEs <sup>a</sup>		
Intraresidue	157	
Sequential	135	
Medium-range ( $l < 4$ )	13	
Long-range	56	
Total NOEs	361	
Others		
$\phi\phi$	38	
Side-chain dihedrals	15	
Hydrogen bonds <sup>b</sup>	3( $\times$ 2)	
Total number of restraints	420	
Deviations from experimental	(SA) <sup>c</sup>	Lowest energy
RMSD of NOE	0.008 (0.0004)	0.008
NOE violations > 0.25 Å	0	0
Violations > 5°	5.35 (0.88)	4
Deviations from ideal geometry		
Bonds (Å)	0.005 (0.0003)	0.005
Angles (deg.)	0.51 (0.04)	0.50
Impropers (deg.)	0.36 (0.017)	0.34
Precision		
RMSD (N, C <sup>z</sup> , C') <sup>d</sup>	0.55 (0.19)	
RMSD (heavy atoms) <sup>d</sup>	1.18 (0.12)	
RMSD (N, C <sup>z</sup> , C') <sup>e</sup>	0.94 (0.25)	
RMSD (heavy atoms) <sup>e</sup>	1.64 (0.26)	
Structural quality		
Procheck (%; mf/aa/ga/da) <sup>f</sup>	54/35/8/3	56/33/9/2
CNS energy <sup>g</sup>	155.4 (7.9)	142.0

<sup>a</sup> Trivial NOE distances were not included and no pseudo atoms were used.

<sup>b</sup> Hydrogen bonds were included as restraints of 2.4 Å between HN and O atoms and 3.3 Å between N and O atoms for the residues involved in the  $\beta$ -sheet.

<sup>c</sup> Average values from 20 lowest-energy structures.

<sup>d</sup> Calculated over residues 334-340 and 345-377.

<sup>e</sup> Calculated over residues 331-378.

<sup>f</sup> Procheck analysis: mf, most favored; aa, additionally allowed; ga, generously allowed; da, disallowed.

<sup>g</sup> Energy calculated from CNS version 1.0.

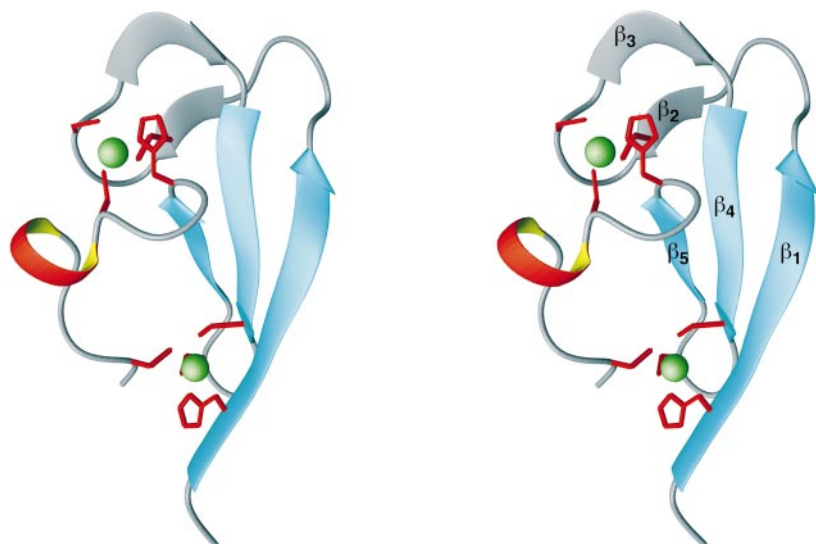


**Figure 1.** Stereo-ribbon diagram of the KSR1 C1 domain. The cysteine and histidine residues involved in  $Zn^{2+}$  coordination are shown as red sticks and the Zn ions are depicted as green spheres. Assignments of the  $\beta 2$  and  $\beta 3$  strands in the hairpin structure (colored in gray) and the C-terminal helix turn were made based on  $\phi, \psi$  angles from the CNS calculations.

$\beta 4$  (residues 355-359) and  $\beta 5$  (residues 364-366). The second  $\beta$ -sheet contains two strands  $\beta 2$  (residues 345-346) and  $\beta 3$  (residues 351-353), and is part of a hairpin structure positioned above the core  $\beta$ -sheet. The helix turn follows the last  $\beta$ -strand and is located between residues 371 and 373. The structure of the KSR1 C1 domain was well defined by the experimental data except for regions displaying a high degree of flexibility, which included residues at the extreme N and C termini, and residues located in the loop between  $\beta 1$  and  $\beta 2$ . (Figure 2(a)).

The KSR1 C1 domain coordinates two molecules of Zn, and the binding sites for the Zn ions are formed by two sets of non-contiguous residues located at either end of the core  $\beta$ -sheet. The helix turn following the  $\beta 5$  strand packs against the  $\beta 1$  strand such that the N and C termini of the C1 domain are brought into close proximity to form one binding site consisting of residues H334, C359, C362, and C377. The second Zn ion is coordinated by residues C346, C349, H367 and C370, and functions to hold the hairpin structure, which includes the  $\beta 2$  and  $\beta 3$  strands, towards the core  $\beta$ -sheet. Due to this configuration, binding of the Zn ions is absolutely required for maintaining the overall structural integrity of the C1 domain.

Strikingly, the core  $\beta$ -sheet of the KSR1 C1 domain exhibits a distinct amphipathic character (Figure 3(a)). The surface that faces the Zn-binding sites and contains residues F336, V357 and L364 is hydrophobic, while the opposite surface, which faces away from the core structure and includes residues K339, K358, and K365, is hydrophilic. In addition to these charged residues in the core  $\beta$ -sheet, other hydrophilic residues (K360, R363, K369 and K372) are scattered throughout the loop and helix regions with their side-chains pointed away from the core structure. As a result, the lower two-thirds of the protein surface is composed largely of positively charged residues (Figure 3(a)). Located

at the top of the C1 domain is a local hydrophobic region formed by residues in the hairpin structure; namely, L342, V345, M353, I354 and F355. These hydrophobic residues constitute the predicted ligand-binding pocket of the KSR1 C1 domain (Figure 3(a)).

### Structural comparison of the KSR1, Raf-1 and PKC $\gamma$ C1 domains

The KSR1 C1 domain is only the second atypical C1 domain whose structure has been determined; the first being that of the Raf-1 kinase.<sup>14</sup> Structures of these two atypical C1 domains together with the structure of the typical PKC $\gamma$  C1b domain<sup>15</sup> are shown in Figure 2. All three domains have a similar overall topology with an identical  $Zn^{2+}$  coordination scheme. It is notable that the core  $\beta$ -sheet of the KSR1 C1 domain is less twisted than that of the Raf-1 and PKC $\gamma$  C1 domains. The KSR1 domain contains more positively charged residues (K339, K358 and K365, K360 and R363) on the hydrophilic side of the  $\beta 1$  sheet than does the Raf-1 and PKC $\gamma$  domains, and it is likely that the electrostatic repulsion between these charged groups accounts for the less twisted conformation of the KSR1 core  $\beta$ -sheet (Figure 2(b)). Overall, the KSR1 C1 domain contains more positively charged residues on its surface than does either the Raf-1 or PKC C1 domains, and these charged residues may facilitate the interaction of the KSR1 C1 domain with acidic phospholipid headgroups present in the plasma membrane. As expected, the most apparent differences between the typical and atypical C1 domains are in the predicted ligand-binding loops located between the  $\beta 1$  and  $\beta 2$  strands ( $\beta 1$ - $\beta 2$  loop) and the  $\beta 3$  and  $\beta 4$  strands ( $\beta 3$ - $\beta 4$  loop) of the hairpin structure. For typical C1 domains, this is the region that mediates binding to phorbol esters and diacylglycerol, and in solution structures of PKC typical C1 domains, both the  $\beta 1$ - $\beta 2$  and the

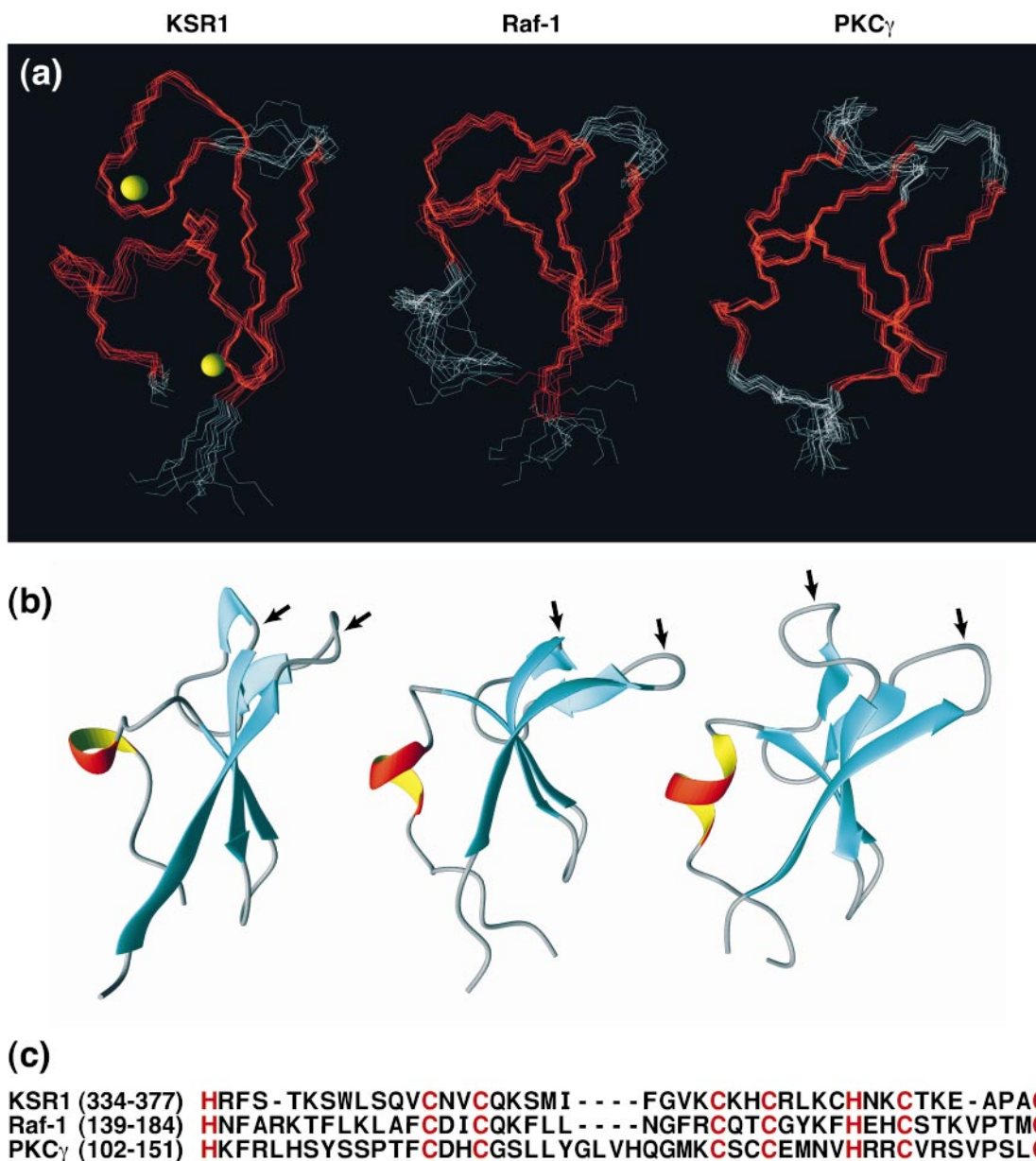


**Figure 2.** Comparison of the KSR1, Raf-1, and PKC $\gamma$  C1 domains. (a) Protein backbone superposition of 11 lowest-energy structures of the KSR1 C1 (residues 331-378), Raf-1 C1 (residues 136-187;<sup>14</sup> Protein Data Bank accession code 1FAQ), and PKC $\gamma$  C1b domains (residues 100-153;<sup>15</sup> Protein Data Bank accession code 1TBO). The flexible regions containing residues with large RMSD values are colored in white. The two Zn ions coordinated in the KSR1 C1 domain are depicted as yellow spheres. (b) Ribbon diagram of the KSR1, Raf-1 (Protein Data Bank accession code 1FAR), and PKC $\gamma$  C1b (Protein Data Bank accession code 1TBN) domains. Arrows indicate the loops predicted to be involved in ligand binding. (c) Amino acid sequences of the KSR1, Raf-1, and PKC $\gamma$  C1b domains. The conserved cysteine and histidine residues that coordinate the Zn ions are shown in red.

$\beta$ 3- $\beta$ 4 loops are flexible.<sup>15-17</sup> In contrast, only the  $\beta$ 1- $\beta$ 2 loop is flexible in the KSR1 and Raf-1 atypical C1 domains; the  $\beta$ 3- $\beta$ 4 loop is immobilized due to a deletion. By mutagenesis studies, the corresponding four residues that are deleted in the atypical C1 domains have been shown to be required for the binding of typical C1 domains to phorbol esters.<sup>13</sup> Thus, both Raf-1 and KSR1 lack the consensus residues in the  $\beta$ 3- $\beta$ 4 loop required for phorbol binding. Consistent with this observation,

we find that the KSR1 C1 domain does not demonstrate high-affinity binding to phorbol esters *in vitro* (data not shown).

The KSR1 C1 domain is most closely related in sequence to the Raf-1 atypical C1 domain, and the length of the predicted ligand-binding loops is similar. However, the three-dimensional structure of the KSR1 domain differs from the Raf-1 domain in this region. For the KSR1 C1 domain, both the  $\beta$ 1- $\beta$ 2 and  $\beta$ 3- $\beta$ 4 loops extend away from the core

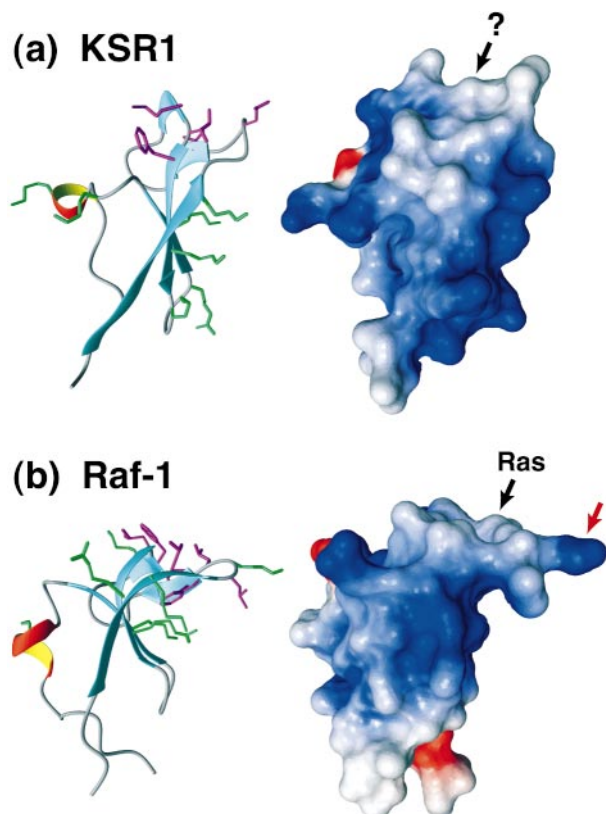


**Figure 3.** Comparison of the predicted ligand binding regions of the atypical KSR1 (a) and Raf-1 (b) C1 domains. Ribbon diagrams are depicted on the left with the side-chains of hydrophobic residues shown in magenta and the side-chains of hydrophilic residues shown in green. Surface charge diagrams are shown on the right with positive charges in blue, negative charges in red, and neutral charges in white. The diagrams were generated by MOLMOL.<sup>51</sup> A red arrow indicates the positively charged lysine residue found in the  $\beta 1$ - $\beta 2$  loop of the Raf-1 C1 domains and black arrows indicate the Ras-binding site of the Raf-1 C1 domain, and the predicted ligand-binding region of the KSR1 C1 domain.

$\beta 1$  sheet, forming a cleft lined with hydrophobic residues (L342, V345, M353, I354, and F355; Figure 3(a)). In contrast, the analogous loops of the Raf-1 C1 domain bend back towards the core  $\beta 1$  sheet, resulting in a more flattened hydrophobic surface (Figure 3(b)). A clear difference is also seen in the amino acid composition of the  $\beta 1$ - $\beta 2$  loop. While only neutral and hydrophobic residues are found in the KSR1  $\beta 1$ - $\beta 2$  loop, the Raf-1  $\beta 1$ - $\beta 2$  loop contains a positively charged hydrophilic residue (K148) that disrupts the hydrophobic pattern of this region (Figure 3(a) and (b)). This hydrophilic lysine residue (K148) as well as other residues within the ligand-binding region of the Raf-1 C1 domain (residues 148-150, 158-160) have been implicated in the Ras/Raf-1 interaction.<sup>18</sup> Previous studies have shown that, in addition to the Ras-binding domain of Raf-1 (residues 51-131 of Raf-

1<sup>9</sup>), the C1 domain is a second region of Raf-1 that contacts Ras directly.<sup>18,20-24</sup> KSR1 proteins, however, have not been found to associate with Ras,<sup>8</sup> and we have not detected an interaction between the KSR1 C1 domain and Ras (data not shown), suggesting that the binding specificities of these atypical C1 domains are not equivalent. Thus, the structural differences in the ligand-binding loops of the atypical C1 domains are likely to contribute to the individual binding specificities of these proteins.

### Functional comparison of the KSR1, Raf-1 and PKC $\gamma$ C1 domains: examination of Raf-1 chimeric proteins

The generation of chimeric proteins in which the endogenous C1 domain of a protein is replaced with C1 sequences from another molecule has been successfully used to examine the function of individual C1 domains.<sup>24,25</sup> Therefore, to address whether the structural distinctions observed between the KSR1, Raf-1, and PKC $\gamma$  C1 domains correlate with functional differences, we constructed chimeric proteins in which the Raf-1 C1 domain was replaced with either the typical C1b domain of PKC $\gamma$  (RPR/Raf-1) or the atypical C1 domain of KSR1 (RKR/Raf-1). We then generated recombinant adenoviruses expressing either the wild-type (WT) or chimeric Raf-1 proteins (Figure 4(a)), infected NIH/3T3 cells with the recombinant adenoviruses, and examined the kinase activity of the Raf-1 proteins. As shown in Figure 4(b), all of the proteins were well expressed; however, they demonstrated dramatically different enzymatic activities in response to various stimuli. As previously reported,<sup>24</sup> the RPR/Raf-1 exhibited a higher basal activity than WT/Raf-1 (1.7-fold higher), but was significantly reduced in its ability to be activated by platelet-derived growth factor (PDGF) treatment (4.9-fold *versus* 15-fold). The activity of RKR/Raf-1 was similar to that of RPR/Raf-1 under these conditions, in that RKR/Raf-1 also had an elevated basal activity (2.3-fold over WT) and a reduced activation following PDGF treatment (only a fivefold activation). Strikingly, in response to 12-*O*-tetradecanoyl-phorbol-13-acetate (TPA) addition, the activation of RPR/Raf-1 was significantly higher than that observed for WT/Raf-1, while the activation of RKR/Raf-1 was again reduced. Thus, the activation response of the WT and chimeric proteins appears to reflect the binding capabilities of the C1 domains, in that the chimeric protein containing the PKC $\gamma$  C1b domain capable of binding phorbol ester had the highest response to TPA, and only the WT/Raf-1 protein containing the C1 domain able to interact with Ras was fully activated by Ras-dependent signals.

Previous studies have shown that the greater activation of RPR/Raf-1 by TPA reflects the ability of the PKC $\gamma$ C1b domain to interact with phorbol esters directly, resulting in the direct recruitment of RPR/Raf-1 to the plasma membrane by TPA.<sup>24</sup> The

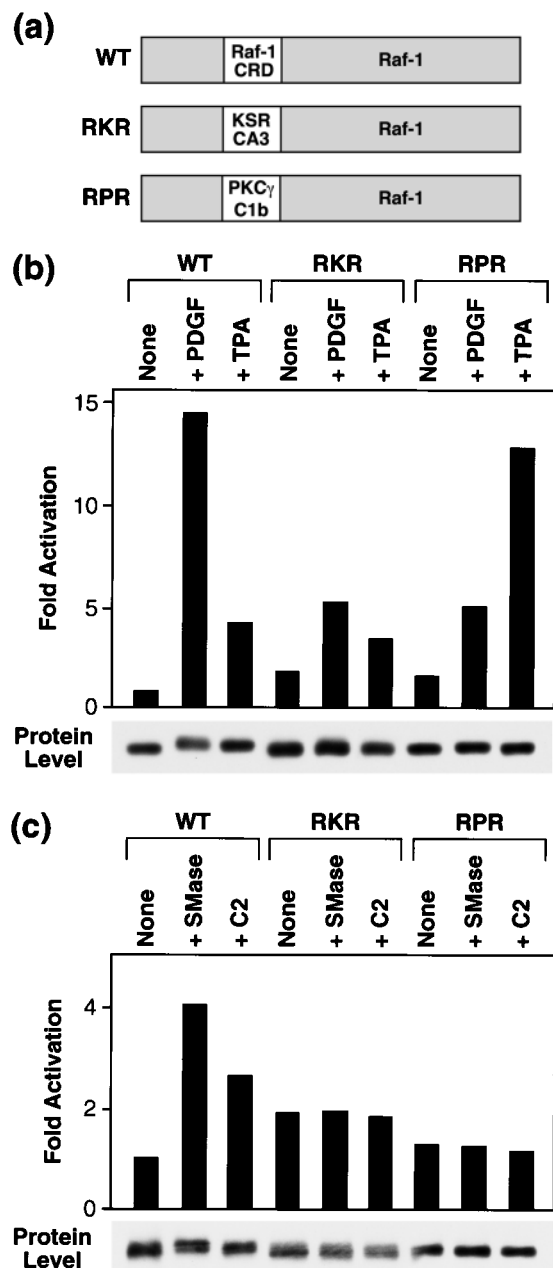


**Figure 4.** Functional analysis of Raf-1 chimeric proteins containing the C1 domains of KSR1 and PKC $\gamma$ . (a) A depiction of the WT, RKR and RPR chimeric Raf-1 proteins. (b) Serum-starved, adenovirus-infected NIH/3T3 cells were left untreated (none) or were treated with PDGF or TPA. Cells were then lysed and the Raf-1 proteins were immunoprecipitated from the lysates using FLAG antibody. The Raf-1 immunoprecipitates were washed extensively and *in vitro* kinase assays were performed. Labeled proteins were separated by SDS-PAGE, transferred to nitrocellulose, and the radioactivity incorporated into kinase inactive MEK determined by phosphor-imager analysis. The membrane was then probed with FLAG antibody to verify the expression level of the Raf-1 proteins. Similar results were obtained in three independent assays. (c) Same as in (b) except cells were left untreated (none) or were treated with sphingomyelinase (SMase) or C2 ceramide (C2). Similar results were obtained in three independent assays.

activation of WT/Raf-1 by TPA, however, has been demonstrated to occur through Ras-dependent mechanisms<sup>26</sup> and results in the membrane localization and activation of only a small percentage of the total Raf-1 protein.<sup>27</sup> Since all of the RPR/Raf-1 proteins would be capable of interacting with TPA, potentially more chimeric molecules could be recruited to the membrane, explaining the greater activation of RPR/Raf-1 than observed for WT/Raf-1. The higher basal activity of both chimeric Raf-1 proteins also supports previous findings, that the Raf-1 C1 domain acts as an autoinhibitory domain in the absence of activating signals.<sup>28,29</sup> The Raf-1 C1 domain mediates this effect by repressing the activity of the Raf-1 kinase domain through intramolecular interactions. Therefore, the increased basal activity of chimeric proteins suggests that these autoinhibitory interactions cannot be mediated by either the KSR1 or PKC $\gamma$  C1 domains. Similarly, the reduced activation of the chimeras in response to PDGF treatment also reflects the binding specificity of the Raf-1 C1 domain and supports the observation that interactions between the C1 domain and Ras are required for full Ras-dependent activation of Raf-1.<sup>23,24</sup> As a result, neither the KSR1 or the PKC $\gamma$  C1 domain can functionally compensate for the Raf-1 C1 domain.

Because some proteins containing atypical C1 domains have been reported to bind ceramide and a role for ceramide in KSR1 activation has been suggested,<sup>30,31</sup> we next examined the effect of ceramide on the activity of the Raf-1 chimeric proteins. Adenovirus-infected NIH/3T3 cells were either treated with C2 ceramide or were treated with sphingomyelinase to generate ceramide *in vivo*, and the kinase activity of the Raf-1 proteins was determined. As shown in Figure 4(c), the activity of WT/Raf-1 was stimulated by both sphingomyelinase and C2 addition. In contrast, the activity of RPR/Raf-1 and RKR/Raf-1 did not change following treatment. Based on the direct activation of RPR/Raf-1 by TPA, we would expect that if the KSR1 C1 domain contacted ceramide directly, some change in RKR/Raf-1 activity would have been observed. Thus, these results suggest that the KSR1 C1 domain does not interact with ceramide *in vivo*, consistent with our *in vitro* binding studies that have failed to demonstrate specific binding between the KSR1 C1 domain and [<sup>3</sup>H]ceramide (data not shown). Interestingly, however, our findings are consistent with the model that Raf-1 itself is a ceramide-activated kinase. Raf-1 has been reported to directly interact with and be activated by ceramide.<sup>32</sup> While studies by Huwiler *et al.*<sup>32</sup> did not define the domain of Raf-1 responsible for interaction, our results suggest that the C1 domain may be involved, since only proteins containing the Raf-1 C1 domain were activated by ceramide. In support of the idea that the Raf-1 C1 domain may mediate the interaction with ceramide, PKC proteins containing atypical C1 domains have been found to interact with and become activated by

ceramide. Strikingly, all the C1 domains of the atypical PKCs contain a positively charged hydrophilic residue at an analogous position in the  $\beta 1$ - $\beta 2$  loop of the predicted ligand-binding region, as is found in the Raf-1 C1 domain, but which is lacking in the KSR1 C1 domain. Thus, it is interesting to speculate that perhaps structural similarities in these atypical C1 domains may account for their responsiveness to ceramide. Proof, however, that the Raf-1 C1 domain binds ceramide directly awaits further investigation, and our data do not exclude the possibility that the activation of WT/Raf-1 by ceramide could be mediated by Ras-dependent mechanisms.

### Functional analysis of a KSR1 chimera containing the C1 domain of Raf-1

To determine whether the function of the KSR1 C1 domain could be replaced by another atypical C1 domain, we generated a chimeric KSR1 protein containing the Raf-1 C1 domain (KRK/KSR1; Figure 5(a)). We then examined the resulting chimera for its ability to augment Ras signaling in *Xenopus laevis* oocyte meiotic maturation assays (Figure 5(b)). As reported,<sup>12</sup> expression of WT/KSR1 markedly accelerated Ras-induced oocyte maturation and MAPK activation; however, expression of a KSR1 protein containing mutations in conserved C1 domain cysteine residues (CC-SS/KSR1) was unable to mediate this effect. Likewise, we found that KRK/KSR1 was unable to facilitate Ras-dependent oocyte maturation and MAPK activation, even though it was fully capable of interacting with MEK and 14-3-3, two proteins that constitutively associate with KSR1 (Figure 5(b) and (c)).

Previously, we have shown that a KSR1 protein artificially targeted to the plasma membrane by a myristylation motif is fully capable of transmitting Ras-dependent signals.<sup>12</sup> Further, we have found that mutation of the C1 domain cysteine residues disrupts KSR1 function and prevents the accumulation of KSR1 into membrane fractions following Ras activation.<sup>12</sup> Therefore, we next examined the effect of the C1 domain substitution on the intracellular localization of KSR1. NIH/3T3 cells were infected with recombinant adenoviruses expressing WT/KSR1, KRK/KSR1, and CC-SS/KSR1, and the localization of the proteins was determined by indirect immunofluorescence. As shown in Figure 6, the staining patterns of the WT/KSR1 and KRK/KSR1 proteins were identical in quiescent cells, with both proteins exhibiting a perinuclear staining in the cytoplasm. In response to PDGF treatment, a dramatic change in the localization of WT/KSR1 was observed, with most of the protein being detected at the plasma membrane. In contrast, the localization of KRK/KSR1 protein did not change significantly following PDGF addition and remained predominantly perinuclear. The localization of CC-SS/KSR1 also did not appear to change in response to PDGF treatment; however,

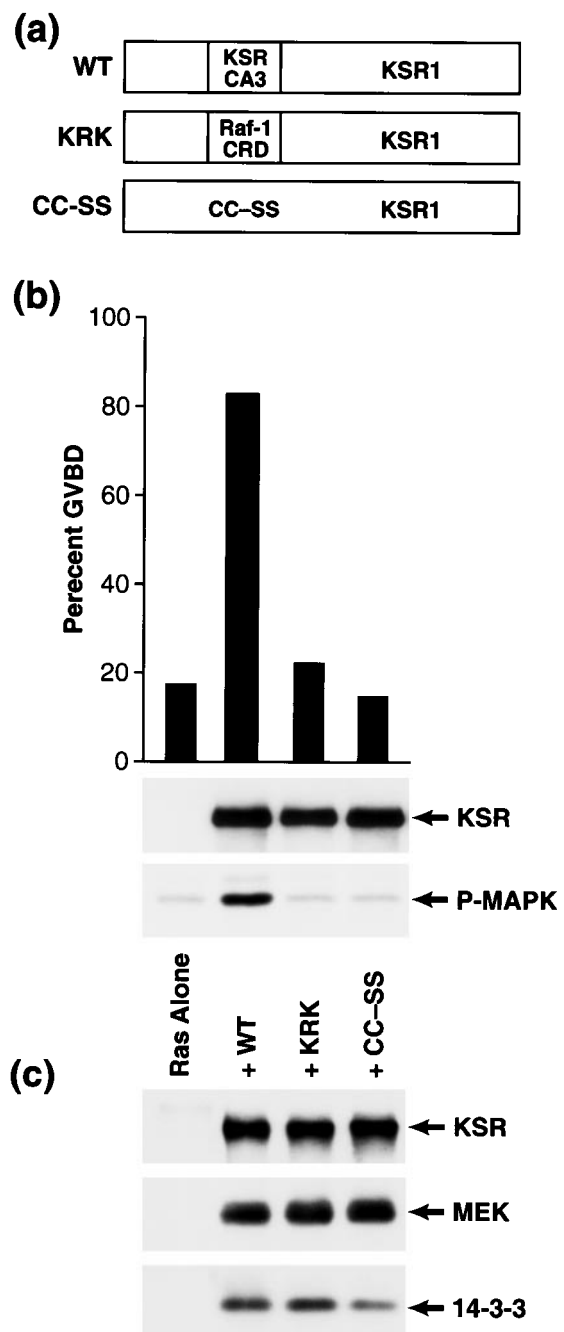


**Figure 5.** Functional analysis of KSR1 proteins containing mutations and substitutions in the C1 domain. (a) A depiction of WT/KSR1, KRK/KSR1, and CC-SS/KSR1 proteins. (b) Meiotic maturation of *Xenopus* oocytes injected with RNA encoding either the WT, KRK, or CC-SS KSR1 and activated Ras<sup>V12</sup>. Germinal vesicle breakdown (GVBD) was scored five hours following Ras injection. Oocyte lysates were prepared and examined by immunoblot analysis using Pyo and phospho-MAPK (P-MAPK) antibodies. Similar results were obtained in two independent assays. (c) KSR1 proteins were immunoprecipitated from oocyte lysates and the immune complexes were examined by immunoblot analysis using Pyo, MEK, and 14-3-3 antibodies.

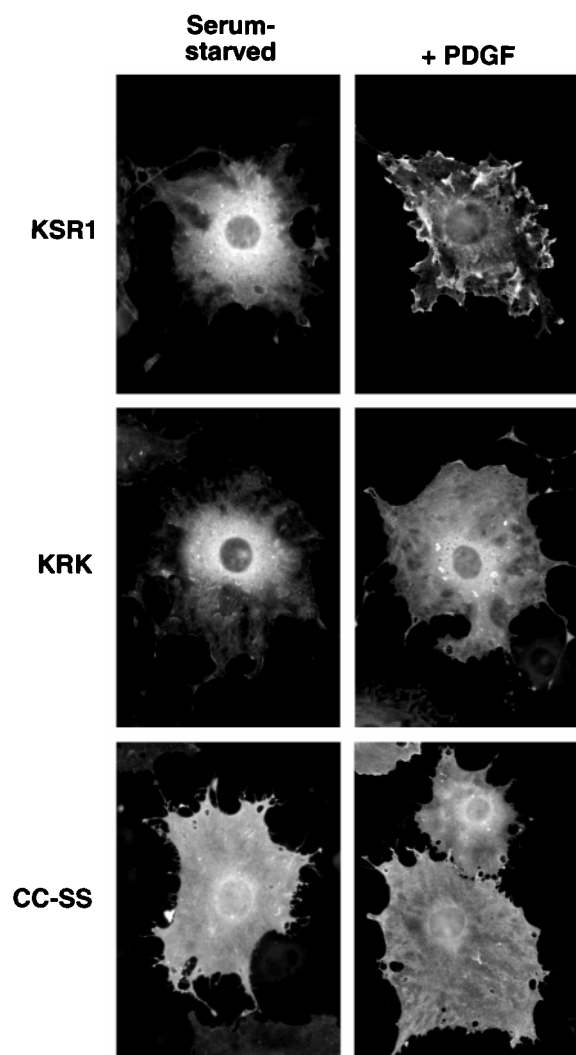


**Figure 6.** The KSR1 C1 domain is required for membrane localization of KSR1 following growth factor treatment. NIH/3T3 cells infected with WT/KSR1 (WT), KRK/KSR1 (KRK) or CC-SS/KSR1 (CC-SS) adenoviruses were left untreated or were treated with PDGF for five minutes. The intracellular localization of the KSR1 proteins was determined by indirect immunofluorescence staining using Pyo antibody.

in both untreated and PDGF-treated cells, diffuse staining was observed throughout the cell. The altered staining pattern of CC-SS/KSR1 apparently is due to the fact that mutation of the conserved cysteine residues disrupts the C1 structure and, as a result, prevents the correct localization of KSR1 in both quiescent and stimulated cells. Interestingly, while substitution of the Raf-1 C1 domain allows for the correct localization of KSR1 in resting cells, it cannot functionally replace the KSR1 C1 domain in mediating the relocalization of KSR1 to the plasma membrane following growth factor

treatment. These findings are consistent with previous studies showing that, while the Raf-1 C1 domain contributes to the membrane association of Raf-1, it is the Ras-binding domain of Raf-1 that is required for translocation.<sup>20–24</sup> As well, mutation of the Raf-1 C1 domain cysteine residues does not prevent the membrane recruitment of Raf-1.<sup>23</sup> Therefore, unlike the Raf-1 C1 domain, our findings demonstrate that the KSR1 C1 domain is essential for the membrane localization of KSR1. The C1 domain presumably mediates the translocation of KSR1 by interacting with distinct membrane-bound ligands.

### Concluding comments

Cysteine-rich C1 domains are found in a variety of proteins involved in signal transduction. These domains mediate interactions with lipids and proteins, which in turn often affects the localization and biological function of their respective proteins. The solution structures of several typical C1 domains from PKC isozymes have been solved,<sup>15–17</sup> along with the crystal structure of PKC $\delta$  C1 complexed with phorbol esters.<sup>33</sup> However, prior to this study, only one atypical C1 structure had been determined, namely that of Raf-1.<sup>14</sup> Atypical C1 domains are more divergent in their primary sequences and do not bind phorbol esters with high affinity. They are found in a variety of proteins including the atypical PKCs, the proto-oncogenes Raf-1 and Vav, and in proteins that have been implicated in small G protein-dependent signaling, including ROCK, Citron, and Lfc.<sup>13</sup> With the solution structure of the KSR1 C1 domain, comparisons can now be made regarding the structures of these domains and their known biological properties. From our analysis, we find that the KSR1 and Raf-1 C1 domains differ significantly in their respective ligand-binding regions. Supporting this finding, Raf-1 and KSR1 chimeric proteins containing swapped C1 sequences demonstrate that these two atypical C1 domains are not interchangeable and instead represent functionally distinct domains that respond to and interact with specific ligands. The chimeric proteins, together with the purified C1 domain of KSR1, are valuable reagents for evaluating potential ligand-binding properties of the KSR1 proteins. In addition, structural comparison of these C1 domains with their known ligand-binding properties provides insight into the residues of each domain that apparently dictate ligand specificity and, as a result, may help to predict the biological activities of novel, uncharacterized C1 domains found in other proteins. Thus, the solution structure of the KSR1 C1 domain, together with those of related C1 domains, will facilitate the interpretation of binding data and help guide further functional characterization of this important regulatory domain.

## Materials and Methods

### Expression and purification of the KSR1 C1 domain

A PCR fragment encoding amino acid residues 331–378 of murine KSR1 preceded by sequences encoding the TEV protease recognition motif<sup>34</sup> was inserted into the pGEX-3X vector (Amersham-Pharmacia). The pGEX-KSR1 C1 domain construct was transformed into BL21/DE3 cells and the bacteria were grown overnight at 37 °C in 100 ml of M9 minimal medium containing 100 µg/ml of ampicillin. The overnight culture was then supplemented with 900 ml of additional medium and grown at 37 °C. ZnCl<sub>2</sub> was added to a final concentration of 5 µM when the A<sub>600</sub> reached 0.3 and isopropyl-β-D-thiogalactopyranoside (IPTG) was added to a final concentration of 0.4 mM when the A<sub>600</sub> reached 0.5. The culture was then allowed to grow at 22 °C for an additional nine hours before the cells were collected by centrifugation. The cell pellet was resuspended in 30 ml of purification buffer (20 mM Tris (pH 7.5), 150 mM NaCl, 0.1 mM sodium citrate, 0.1 mM Tris(2-carboxyethyl)phosphine (TCEP)) and lysed by sonication. The cell lysate was centrifuged at 20,000 g for 30 minutes at 4 °C. The supernatant containing the GST-KSR1 C1 domain protein was then bound to a glutathione-Sepharose 4B column (Amersham-Pharmacia) and the C1 domain cleaved from GST using TEV protease at a 1:100 ratio (molar) of TEV to GST-KSR1 C1.<sup>35</sup> The cleaved C1 domain was then separated from the TEV protease using a Mono S column (Pharmacia Biotech). Proteins binding to the Mono S column were eluted using a 0 to 1 M NaCl gradient in purification buffer that contained 10 µM ZnCl<sub>2</sub>. The KSR1 C1 domain came off the column at a NaCl concentration of approximately 0.5 M. The pure C1 domain was then exchanged into NMR sample buffer (30 mM Tris-acetate (pH 6.5), 100 mM NaCl, 100 mM Na<sub>2</sub>SO<sub>4</sub>, 0.1 mM sodium citrate, 0.1 mM TCEP, 10 µM ZnCl<sub>2</sub>) and concentrated to approximately 1 mM. The purity of C1 protein was confirmed using SDS-PAGE.

### Structure determination

The NMR experiments were performed on a Varian Unity-plus 500MHz or 600 MHz spectrometer equipped with Z-spec triple-resonance probes (Nalorac Corporation) at 25 °C. The data were then processed with NMRPipe<sup>36</sup> and analyzed using ANSIG 3.3.<sup>37</sup> Sequential assignment of <sup>1</sup>H, <sup>15</sup>N and <sup>13</sup>C resonances of the KSR1 C1 domain were made from HSQC, HNCACB,<sup>38</sup> CBCA(CO)NH,<sup>39</sup> C(CO)NH<sup>40</sup> and HCCHTOCSY<sup>41,42</sup> experiments. The side-chain dihedral angles were determined by a qualitative comparison of the intensities in 3D HNHB<sup>43</sup> and HN(CO)HB.<sup>44</sup> The protonation state of the histidine imidazole group was determined using the two-bond coupling pattern observed in a modified HSQC experiment.<sup>14,45</sup> Inter-proton distance restraints were obtained from the NOEs determined by a 3D <sup>15</sup>N-edited NOESY-HSQC (100 ms mixing time), a simultaneous <sup>13</sup>C and <sup>15</sup>N-edited NOESY-HSQC (150 ms mixing time) and a 3D <sup>13</sup>C-edited NOESY-HSQC in <sup>2</sup>H<sub>2</sub>O (150 ms mixing time).

### Structure calculations

Structures were calculated using CNS version 1.0<sup>46</sup> on an R10000-based multiprocessor SGI Power Challenge. The NOE distance restraints were converted from the NOE peak volumes in the spectra by using an internal

calibration (strong 2.2 Å; medium 3.2 Å; weak 4.5 Å). The protein backbone torsion angles were generated by TALOS<sup>47</sup> based upon the chemical shifts of H<sup>α</sup>, C<sup>α</sup> and C<sup>β</sup>. The hydrogen bond restraints were identified from NOE patterns between residues and by comparison to Raf-1<sup>14</sup> and PKCγ<sup>15</sup> C1 domain structures. A total of 361 unambiguous NOEs, 38 pairs of φ,ψ torsion angles, 15 side-chain dihedral restraints, and three hydrogen bond restraints were initially used to generate the structures. The expected Zn<sup>2+</sup> coordination sites were clearly formed in the absence of any explicit restraints. Two Zn<sup>2+</sup> atoms were then incorporated into the structure with the NOE distance restraints of 2.3 Å for Zn-S and 2.0 Å for Zn-N.<sup>47</sup> The Zn ion coordinations were tetrahedrally constrained (109° for the angles of S-Zn-S and N-Zn-S)<sup>49,50</sup> and the residues involved in Zn<sup>2+</sup> binding agree with the Raf-1 and PKC C1 domain structures. A fully extended and energy-minimized conformation of the KSR1 C1 polypeptide was used as the starting structure. The CNS molecular dynamics calculations basically contained four stages.<sup>46</sup> The first stage consisted of dynamic heating of 4000 steps at 40000 K with 0.015 ps increment. The second stage consisted of 2000 steps of the torsion angle dynamic cooling from 10000 K to 300 K, followed by the third stage of 1000 cooling steps of Cartesian molecular dynamics from 300 K to 100 K. The fourth stage consisted of 3000 steps of conjugated-gradient energy minimization. The calculations generated good convergence, and 20 lowest-energy structures were chosen for further analysis and for quality examination on MOLMOL<sup>51</sup> and PROCHECK.<sup>52</sup>

### Construction of chimeric Raf-1 and KSR1 proteins and generation of recombinant adenoviruses

KSR1 and Raf-1 constructs containing C1 domains swaps were generated in two steps. First, a PCR fragment encoding the C1 domain of Raf-1 (residues 137–184) flanked by 5' and 3' sequences of KSR1 (encoding residues 322–331 and 378–387, respectively) and a fragment encoding the C1 domain of KSR1 (residues 332–377) flanked by 5' and 3' sequences of Raf-1 (encoding residues 127–136 and 185–194, respectively) were generated. In the second step, the KSR1 C1 domain fragment containing the Raf-1 sequence overhang and the Raf-C1 domain fragment containing the KSR1 sequence overhang were used as primers in the QuikChange site-directed mutagenesis protocol (Stratagene) to generate constructs encoding the RKR/Raf-1 and KRK/KSR1 chimeric proteins, respectively. All constructs were confirmed by DNA sequencing. The RPR/Raf-1 construct in which the Raf-1 C1 domain was replaced with the C1b domain of PKCγ<sup>24</sup> was obtained from Dr Joseph Avruch at the Harvard Medical School. All the Raf-1 proteins were constructed to contain an N-terminal FLAG epitope tag, while the KSR1 proteins contained an N-terminal polyoma tag. Sequences encoding WT and the chimeric Raf-1 and KSR1 proteins were subcloned into the pSP64Ten vector for the synthesis of RNA *in vitro* or were inserted into the pAD-Track-CMV vector for the production of recombinant adenoviruses. Recombinant adenoviruses were then generated as described.<sup>53</sup>

### Protein expression using recombinant adenoviruses

NIH/3T3 cells were plated in growth medium containing Dulbecco's modified Eagle medium (DMEM) supplemented with 10% (v/v) fetal bovine serum (FBS)

at a concentration of  $1.2 \times 10^6$  cells per 10 cm dish and grown at 37°C in 5% CO<sub>2</sub>. At 18 hours after plating, the growth medium was removed and the cells were incubated in infection medium containing 5 ml of OPTI-MEM (Invitrogen) medium, 10 µl of LipofectA-MINE (Invitrogen) and aliquots of the desired adenovirus. After incubation for two hours at 37°C, the infection medium was removed and growth medium was added to each plate. Cells were then incubated at 37°C in 5% CO<sub>2</sub> and serum-starved for 18 hours prior to stimulation with mitogens or growth factors. Cells were treated with 50 ng/ml of PDGF for five minutes, with 1 µM TPA, 50 µM C2 ceramide or 10 milli-units/ml of sphingomyelinase for 15 minutes at 37°C.

### Cell lysis, immunoprecipitation, and kinase assays

Stimulated cells were washed twice with ice-cold PBS buffer and lysed for 15 minutes at 4°C in radioimmunoprecipitation assay lysis buffer (RIPA) containing 20 mM Tris (pH 8.0), 137 mM NaCl, 10% (v/v) glycerol, 1% (v/v) Nonidet P-40, 0.1% (w/v) SDS, 0.5% (w/v) sodium deoxycholate, 2 mM EDTA, 1 mM phenylmethylsulfonyl fluoride, aprotinin (0.15 unit/ml), 20 µM leupeptin and 5 mM sodium vanadate. The insoluble material was removed by centrifugation at 4°C for 20 minutes at 16,000 g. For immunoprecipitation assays, the lysates were incubated with the appropriate antibody and Protein G beads for four hours at 4°C. The samples were then washed three times with Nonidet P-40 lysis buffer (20 mM Tris (pH 8.0), 137 mM NaCl, 10% glycerol, 1% Nonidet P-40, 2 mM EDTA) and either analyzed directly or were incubated at 25°C for 30 minutes in 40 µl of kinase buffer (30 mM Tris (pH 7.4), 10 mM MnCl<sub>2</sub>, 1 mM DTT, 5 µM ATP) containing 20 µCi of [ $\gamma$ -<sup>32</sup>P]ATP and 0.1 µg of purified kinase inactive MEK1. Kinase assays were terminated by the addition of gel loading buffer (50 mM Tris (pH 6.8), 2% SDS, 100 mM DTT, 10% glycerol, 0.1% (w/v) bromophenol blue). The samples were resolved by SDS-PAGE and phosphoproteins were visualized and quantified using a phosphor-imager (Molecular Dynamics).

### RNA transcription, oocyte injection and analysis

Capped RNA was transcribed using the mMessage mMachine Sp6 kit (Ambion). Buffer or RNA (30 ng) encoding the various KSR1 constructs was injected into stage VI oocytes as described.<sup>7</sup> After approximately 12 hours, the oocytes were injected with Ras<sup>V12</sup> RNA and were subsequently scored for germinal vesicle breakdown (GVBD), as evidenced by the appearance of a white spot at the animal pole. For biochemical analysis, oocytes were lysed (10 µl of RIPA buffer per oocyte) by trituration with a pipette tip. Lysates were cleared by centrifugation at 14,000 g for five minutes at 4°C.

### Immunofluorescence

NIH/3T3 cells seeded onto 18 mm glass coverslips were infected with the appropriate KSR1 adenovirus. At 48 hours after infection, serum-starved cells were either left untreated or were treated for five minutes with PDGF. Cells were then washed once with phosphate buffered saline (PBS) and fixed in freshly prepared 4% (v/v) paraformaldehyde/PBS for ten minutes at 25°C. Following two washes with PBS, the cells were permeabilized for five minutes with 0.1% Triton X-100 in PBS.

The cells were washed again with PBS and blocked for one hour in 3% (w/v) bovine serum albumin (BSA) in PBS. Following an incubation for one hour at 25°C in the appropriate antibody, the cells were washed four times with PBS and incubated with either anti-mouse or anti-rabbit Alexa dye secondary antibody (Molecular Probes) diluted 1:1000 in blocking buffer for 45 minutes at 25°C, protected from light. After four more washes in PBS, the coverslips were washed in distilled water and mounted in Prolong antifade medium (Molecular Probes).

### Data deposition

Resonance assignments have been deposited in the BioMag Res Bank (BMRB: accession code 5203). The structural coordinates have been deposited in the RCSB Protein Data Bank (accession code 1KBE, lowest-energy structure; 1KBF, 20 refined structures).

### Acknowledgments

We thank members of the Morrison, Byrd, and Waugh laboratories for helpful comments and suggestions. In addition, we thank Sergey Tarasov, Eric Anderson, Sharon Campbell, and Jason William for technical advice and Dan Ritt for excellent technical assistance. We acknowledge the NCI-Frederick Biomedical supercomputing Center for the use of computational resources.

©2002 US Government

### References

1. Kolch, W. (2000). Meaningful relationships: the regulation of the Ras/Raf/MEK/ERK pathway by protein interactions. *Biochem. J.* **351**, 289-305.
2. Therrien, M., Chang, H. C., Solomon, N. M., Karim, F. D., Wassarman, D. A. & Rubin, G. M. (1995). KSR, a novel protein kinase required for RAS signal transduction. *Cell*, **83**, 879-888.
3. Kornfeld, K., Hom, D. B. & Horvitz, H. R. (1995). The *ksr-1* gene encodes a novel protein kinase involved in Ras-mediated signaling in *C. elegans*. *Cell*, **83**, 903-913.
4. Sundaram, M. & Han, M. (1995). The *C. elegans ksr-1* gene encodes a novel Raf-related kinase involved in Ras-mediated signal transduction. *Cell*, **83**, 889-901.
5. Müller, J., Cacace, A. M., Lyons, W. E., McGill, C. B. & Morrison, D. K. (2000). Identification of B-KSR1, a novel brain-specific isoform of KSR1 that functions in neuronal signaling. *Mol. Cell Biol.* **20**, 5529-5539.
6. Stewart, S., Sundaram, M., Zhang, Y., Lee, J., Han, M. & Guan, K.-L. (1999). Kinase suppressor of Ras forms a multiprotein signaling complex and modulates MEK localization. *Mol. Cell Biol.* **19**, 5523-5534.
7. Therrien, M., Michaud, N. R., Rubin, G. M. & Morrison, D. K. (1996). KSR modulates signal propagation within the MAPK cascade. *Genes Dev.* **10**, 2684-2695.
8. Denouel-Galy, A., Douville, E. M., Warne, P. H., Papin, C., Laugier, D., Calothy, G. *et al.* (1997). Murine Ksr interacts with MEK and inhibits Ras-induced transformation. *Curr. Biol.* **8**, 46-55.

9. Xing, H., Kornfeld, K. & Muslin, A. J. (1997). The protein kinase KSR interacts with 14-3-3 protein and Raf. *Curr. Biol.* **7**, 294-300.
10. Yu, W., Fantl, W. J., Harrowe, G. & Williams, L. T. (1997). Regulation of the MAP kinase pathway by mammalian KSR through direct interaction with MEK and ERK. *Curr. Biol.* **8**, 56-64.
11. Morrison, D. K. (2001). KSR: a MAPK scaffold of the Ras pathway? *J. Cell Sci.* **114**, 1609-1612.
12. Michaud, N. R., Therrien, M., Cacace, A., Edsall, L. C., Spiegel, S., Rubin, G. M. & Morrison, D. K. (1997). KSR stimulates Raf-1 activity in a kinase-independent manner. *Proc. Natl Acad. Sci. USA*, **94**, 12792-12796.
13. Hurley, J. H., Newton, A. C., Parker, P. J., Blumberg, P. M. & Nishizuka, Y. (1997). Taxonomy and function of C1 protein kinase C homology domains. *Protein Sci.* **6**, 477-480.
14. Mott, H. R., Carpenter, J. W., Zhong, S., Ghosh, S., Bell, R. M. & Campbell, S. L. (1996). The solution structure of the Raf-1 cysteine-rich domain: a novel Ras and phospholipid binding site. *Proc. Natl Acad. Sci. USA*, **93**, 8312-8317.
15. Xu, R. X., Pawelczyk, T., Xia, T. H. & Brown, S. C. (1997). NMR structure of a protein kinase C- $\gamma$  phorbol-binding domain and study of protein-lipid micelle interactions. *Biochemistry*, **36**, 10709-10717.
16. Hommel, U., Zurini, M. & Luyten, M. (1994). Solution structure of a cysteine rich domain of rat protein kinase C. *Nature Struct. Biol.* **1**, 383-387.
17. Ichikawa, S., Hatanaka, H., Takeuchi, Y., Ohno, S. & Inagaki, F. (1995). Solution structure of cysteine-rich domain protein kinase C $\alpha$ . *J. Biochem.* **117**, 566-574.
18. Williams, J. G., Drugan, J. K., Yi, G.-S., Clark, G. J., Der, C. J. & Campbell, S. L. (2000). Elucidation of binding determinants and functional consequences of Ras/Raf-cysteine-rich domain interactions. *J. Biol. Chem.* **275**, 22172-22179.
19. Vojtek, A. B., Hollenberg, S. M. & Cooper, J. A. (1993). Mammalian Ras interacts directly with the serine/threonine kinase Raf. *Cell*, **74**, 205-214.
20. Brtva, T. R., Drugan, J. K., Gosh, S., Terrell, R. S., Campbell-Burk, S., Bell, R. M. & Der, C. J. (1995). Two distinct Raf domains mediate interaction with Ras. *J. Biol. Chem.* **270**, 9809-9812.
21. Hu, C. D., Kariya, K., Tamada, M., Akasada, K., Shirouzu, M., Yokoama, S. & Kataoka, T. (1995). Cysteine-rich region of Raf-1 interacts with activator domain of post-translationally modified Ha-Ras. *J. Biol. Chem.* **270**, 30274-30277.
22. Drugan, J. K., Khosravi-Far, R., White, M. A., Der, C. J., Sung, Y. J., Hwang, Y. W. & Campbell, S. L. (1996). Ras interaction with two distinct binding domains in Raf-1 may be required for Ras activation. *J. Biol. Chem.* **271**, 233-237.
23. Roy, S., Lane, A., Yan, J., McPherson, R. & Hancock, J. F. (1997). Activity of plasma membrane-recruited Raf-1 is regulated by Ras via the Raf zinc finger. *J. Biol. Chem.* **272**, 20139-20145.
24. Luo, A., Diaz, B., Marshall, M. S. & Avruch, J. (1997). An intact Raf zinc finger is required for optimal binding to processed Ras and Ras-dependent Raf activation *in situ*. *Mol. Cell. Biol.* **17**, 46-53.
25. Schmitz, H.-P., Jockel, J., Block, C. & Heinsch, J. J. (2001). Domain shuffling as a tool for investigation of protein function: substitution of the cysteine-rich region of Raf kinase and PKC $\eta$  for that of yeast Pkc1p. *J. Mol. Biol.* **311**, 1-7.
26. Marais, R., Light, Y., Mason, C., Paterson, H., Olson, M. F. & Marshall, C. J. (1998). Requirement of Ras-GTP-Raf complexes for activation of Raf-1 by protein kinase C. *Science*, **280**, 109-112.
27. Hallberg, B., Rayter, S. I. & Downward, J. (1994). Interaction of Ras and Raf in intact mammalian cells upon extracellular stimulation. *J. Biol. Chem.* **269**, 3913-3916.
28. Cutler, R. E., Jr, Stephens, R. M., Sarcino, M. R. & Morrison, D. K. (1998). Autoregulation of the Raf-1 serine/threonine kinase. *Proc. Natl Acad. Sci. USA*, **95**, 9214-9219.
29. Winkler, D. G., Cutler, R. E., Jr, Drugan, J. K., Campbell, S., Morrison, D. K. & Cooper, J. A. (1998). Identification of residues in the cysteine-rich domain of Raf-1 that control Ras binding and Raf-1 activity. *J. Biol. Chem.* **273**, 21578-21584.
30. Zhang, Y., Yao, B., Delikat, S., Bayoumy, S., Lin, X.-H., Basu, S. *et al.* (1997). Kinase suppressor of Ras is ceramide-activated protein kinase. *Cell*, **89**, 63-72.
31. van Blitterswijk, W. J. (1998). Hypothesis: ceramide conditionally activates atypical protein kinases C, Raf-1 and KSR through binding to their cysteine-rich domains. *Biochem. J.* **331**, 679-80.
32. Huwiler, A., Brunner, J., Hummel, R., Vervoordeldonk, M., Stabel, S., van den Bosch, H. & Pfeilschifter, J. (1996). Ceramide-binding and activation defines protein kinase cRaf as a ceramide-activated protein kinase. *Proc. Natl Acad. Sci. USA*, **93**, 6959-6956.
33. Zhang, G., Kazanietz, M. G., Blumberg, P. M. & Hurley, J. H. (1995). Crystal structure of the cys2 activator-binding domain of protein kinase C delta in complex with phorbol ester. *Cell*, **81**, 917-924.
34. Parks, T. D., Leuther, K. K., Howard, E. D., Johnston, S. A. & Dougherty, W. G. (1994). Release of proteins and peptides from fusion proteins using a recombinant plantvirus proteinase. *Anal. Biochem.* **216**, 413-417.
35. Kapust, R. B. & Waugh, D. S. (2000). Controlled intracellular processing of fusion proteins by TEV protease. *Protein Expr. Purif.* **19**, 312-318.
36. Delaglio, F., Grzesiek, S., Vuister, G. W., Zhu, G., Pfeifer, J. & Bax, A. (1995). NMRPipe: a multidimensional spectral processing system based on UNIX pipes. *J. Biomol. NMR*, **6**, 277-293.
37. Kraulis, P. J. (1989). ANSIG: a program for the assignment of protein 1H 2D NMR spectra by interactive computer graphics. *J. Magn. Reson.* **84**, 627-633.
38. Wittekind, M. & Mueller, L. (1993). HNCACB, a high-sensitivity 3D NMR experiment to correlate amide-proton and nitrogen resonances with the alpha- and beta-carbon resonances in proteins. *J. Magn. Reson. ser. B*, **101**, 201-205.
39. Grzesiek, S. & Bax, A. (1992). Correlating backbone amide and side-chain resonances in larger proteins by multiple relayed triple resonance NMR. *J. Am. Chem. Soc.* **114**, 6291-6293.
40. Grzesiek, S., Anglister, J. & Bax, A. (1993). Correlation of backbone amide and aliphatic side-chain resonances in  $^{13}\text{C}/^{15}\text{N}$ -enriched proteins by isotropic mixing of  $^{13}\text{C}$  magnetization. *J. Magn. Reson.* **101**, 114-119.
41. Bax, A., Clore, G. M. & Gronenborn, A. M. (1990).  $^1\text{H}$ - $^1\text{H}$  correlation via isotropic mixing of  $^{13}\text{C}$  magnetization, a new three-dimensional approach for assigning  $^1\text{H}$  and  $^{13}\text{C}$  spectra of  $^{13}\text{C}$  enriched proteins. *J. Magn. Reson.* **88**, 425-431.

42. Kay, L. E., Xu, G. Y., Singer, A. U., Muhandiram, D. R. & Formankay, J. D. (1993). A gradient-enhanced HCCH-TOCSY experiment for recording side-chain  $^1\text{H}$  and  $^{13}\text{C}$  correlations in  $\text{H}_2\text{O}$  samples of proteins. *J. Magn. Reson. ser. B*, **101**, 333-337.
43. Archer, S. J., Ikura, M., Torchia, D. & Bax, A. (1991). An alternative 3D NMR technique for correlating backbone  $^{15}\text{N}$  with side-chain H $\beta$  resonances in larger proteins. *J. Magn. Reson.* **95**, 636-641.
44. Grzesiek, S., Ikura, M., Clore, G. M., Gronenborn, A. M. & Bax, A. (1992). A 3D triple-resonance NMR technique for qualitative measurement of carbonyl-H $\beta$  J couplings in isotropically enriched proteins. *J. Magn. Reson.* **96**, 215-221.
45. Pelton, J. G., Torchia, D. A., Meadow, N. D. & Roseman, S. (1993). Tautomeric states of the active-site histidines of phosphorylated and unphosphorylated III $\text{Glc}$ , a signal-transducing protein from *Escherichia coli*, using two-dimensional heteronuclear NMR techniques. *Protein Sci.* **2**, 543-558.
46. Stein, E. G., Rice, L. M. & Brunger, A. T. (1997). Torsion-angle molecular dynamics as a new efficient tool for NMR structure calculation. *J. Magn. Reson.* **124**, 154-164.
47. Cornilescu, G., Delaglio, F. & Bax, A. (1999). Protein backbone angle restraints from searching a database for chemical shift and sequence homology. *J. Biomol. NMR*, **13**, 289-302.
48. Diakun, G. P., Fairall, L. & Klug, A. (1986). EXAFS study of the zinc-binding sites in the protein transcription factor IIIA. *Nature*, **324**, 698-699.
49. Martinez-Yamout, M., Legge, G. B., Zhang, O., Wright, P. E. & Dyson, H. J. (2000). Solution structure of the cysteine-rich domain of the *Escherichia coli* chaperone protein DnaJ. *J. Mol. Biol.* **300**, 805-818.
50. Lee, M. S., Kliewer, S. A., Provencal, J., Wright, P. E. & Evans, R. M. (1993). Structure of the retinoid X receptor alpha DNA binding domain: a helix required for homodimeric DNA binding. *Science*, **260**, 1117-1121.
51. Koradi, R., Billeter, M. & Wuthrich, K. (1996). MOLMOL: a program for display and analysis of macromolecular structures. *J. Mol. Graph.* **14**, 51-55.
52. Laskowski, R. A., MacArthur, M. W., Moss, D. S. & Thornton, J. M. (1993). PROCHECK: a program to check the stereochemical quality of protein structures. *J. Appl. Crystallog.* **26**, 283-291.
53. He, T.-C., Zhou, S., da Costa, L. T., Yu, J., Kinzler, K. W. & Vogelstein, B. (1998). A simplified system for generating recombinant adenoviruses. *Proc. Natl Acad. Sci. USA*, **95**, 2509-2514.

*Edited by P. E. Wright*

*(Received 1 October 2001; received in revised form 9 November 2001; accepted 13 November 2001)*